Model Sensitivity to Topographic Uncertainty in Meso- and Microtidal Marshes

Karim Alizad, Stephen C. Medeiros, Madeline R. Foster-Martinez, and Scott C. Hagen

***Abstract*—Light detection and ranging (Lidar) derived digital elevation models are widely used in modeling coastal marsh systems. However, the topographic error in these models can affect simulations of marsh coverage and characteristics. We investigated the relevance and impact of this error in micro- and mesotidal systems. Lidar-derived and RTK-adjusted topography were each used in a dynamic marsh model, and the resulting marsh coverages were examined. For two microtidal sites (Apalachicola, FL, USA, and Grand Bay, MS, USA) using solely lidar-derived topography, the model produced Cohen Kappa values of 0.1 for both estuaries when compared with National Wetland Inventory data indicating "very poor agreement." Applying the RTK-adjusted topography improved the model marsh coverage results to "substantial agreement" with the values to 0.6 and 0.77, respectively. The mesotidal site in Plum Island, MA, USA, contained similar topographic errors, but the model produced a Cohen Kappa value of 0.73, which categorized it as "very good agreement" with no need for a further topographic adjustment given its present robust biomass productivity. The results demonstrate that marsh models are sensitive to topographic errors when the errors are comparable to the tidal range. The particular sensitivity of the modeling results to topographic error in microtidal systems highlights the need for close scrutiny of lidar-derived topography.**

***Index Terms*—About hydro-Marsh equilibrium model (MEM), biogeophysical models, digital elevation models, light detection and ranging (lidar).**

I. Introduction

SALT marshes are responsible for positive impacts on coastal ecosystems, including wave energy attenuation, shoreline stabilization, erosion resistance, and nutrient assimilation [4]–[8]. They also provide habitat for numerous species and space for recreational activities. By trapping sediment and increasing the elevation of the marsh platform, marshes can adapt to water-level changes and associated effects, such as erosion and increased inundation from tides and storm surge. This mechanism is enhanced with greater vegetation density, biomass production, and marsh coverage [10]. Yet, this marsh accretion may not be enough to keep pace with accelerated rates of sea-level rise (SLR), as their low topography puts them at particular risk for erosion and permanent inundation [12]. Due to the many services provided by marshes and their dynamic response to SLR, there has been an effort to create models that predict marsh coverage and evolution. These models aim to present actionable information for mitigating marsh loss or to provide restoration planning and coastal management guidance [14].

Most marsh models rely on the principle that the resiliency of coastal salt marshes can be assessed by characterizing their elevation relative to the current tide range [5], [17]. The tide range is defined as the vertical elevation range between mean high water (MHW) and mean low water. Areas of marsh higher in the tidal frame (i.e., above mean sea level) are less threatened by SLR than areas lower in the tidal frame. When the tide range is small, as with microtidal systems (<2 m tide range), there is a smaller vertical difference between these areas, making microtidal marshes less resilient to SLR. Research shows that marshes in a microtidal system are reliant on the allochthonous sediment from storms and flooding to maintain their vertical elevation [20] and tend to expand and retreat more quickly than marshes in a mesotidal (2–4 m) or macrotidal (>2 m) environment [20], [22]. The sensitivity of microtidal marsh systems is especially relevant in the northern Gulf of Mexico (NGOM), where the one-meter elevation contour can extend anywhere from 3 to 10 km inland [24].

Similarly to marsh resiliency, complex interrelationships between physics and biology are often characterized in marsh ecological models by the hydroperiod or the frequency and duration of tidal inundation [26]. These models require the coupling of seemingly disparate models to capture sensitivity and feedback processes [28]. The relationship between topography and hydroperiod is directly, but not exclusively, simulated in salt marsh models, and is largely responsible for marsh productivity and coverage projections [29]–[36]. Both the marsh surface topography and elevation strongly influence the hydroperiod [37].

Manuscript received April 18, 2019; revised January 30, 2020; accepted February 9, 2020. Date of publication February 13, 2020; date of current version March 2, 2020. This work was supported in part by Award NA10NOS4780146 and NA16NOS4780208 from the NOAA, Award EAR1660502 from the NSF and the Louisiana Sea Grant Laborde Chair. The computations for the simulations were performed using the STOKES ARCC at University of Central Florida, the XSEDE, which is supported by the NSF grant number ACI-1053575 [1]. *(Corresponding author: Karim Alizad.)*

Karim Alizad is with the Baruch Institute for Marine and Coastal Sciences, University of South Carolina, Columbia, SC 29208 USA (e-mail: alizad@sc.edu).

Stephen C. Medeiros is with the Department of Civil Engineering, Embry-Riddle Aeronautical University, Daytona Beach, FL 32114 USA (e-mail: medeiros@erau.edu).

Madeline R. Foster-Martinez is with the Pontchartrain Institute for Environmental Sciences, University of New Orleans, New Orleans, LA 70148 USA (e-mail: mrfoster@uno.edu).

Scott C. Hagen is with the Department of Civil and Environmental Engineering, the Center for Computation and Technology, and the Center for Coastal Resiliency, Louisiana State University, Baton Rouge, LA 70808 USA (e-mail: shagen@lsu.edu).

Digital Object Identifier 10.1109/JSTARS.2020.2973490

A. Light Detection and Ranging (Lidar) Error in Marsh Systems

Whether assessing resiliency or modeling ecological productivity, the initial elevation is a critical model input. Considering the large geographic scale of many salt marshes, airborne lidar is often utilized as the primary source of topographic data [38]–[42]. These missions are commonly flown using near-infrared lasers (1064 nm wavelength) at altitudes from 1000 to 3000 m, which produce beam divergences resulting in ground footprint sizes from 0.2 to 0.6 m, respectively [43]. Previous research shows that there is a high bias in the marsh surface elevation obtained from the bare earth lidar-derived digital elevation models (DEMs) [25], [44]–[46]. The bias is largely due to the following four factors. First, less than 0.15 m of bias can be attributed to the inability of the airborne laser to penetrate the dense grasses [15]. Second, the “dead zone” defined as the vegetation structure height that results in only one laser return per pulse can add approximately 0.10 m [19]. Third, the standing water or wet substrates often present on the marsh surface that absorbs the laser pulse [44]. Fourth, the heterogeneity of above-ground biomass density on small spatial scales [47] can bias the results up to an amount equal to the difference between the synoptic water level and the local ground surface elevation. On hard flat surfaces, often referred to as “open terrain,” lidar typically has a root-mean-square error (RMSE) in vertical elevation of less than 10 cm; however, the accepted value for vertical RMSE over all land cover classes is 15 cm. This value is interpreted as an accuracy of ±15 cm [14], [15], [48]. A summary of previous studies examining lidar elevation error in salt marshes is presented in Table I. Taken in aggregate, these studies have a pooled mean lidar error of 18 cm and a standard deviation of 14 cm.

TABLE I
LIDAR ERROR REPORTED IN PREVIOUS SALT MARSH MODELING STUDIES

Study	Location	Lidar Error (m)	Ground Truth Source
Morris, et al. [3]	North Inlet, SC	0.13 ± 0.065	Post Processed GPS
Montane and Torres [9]	North Inlet-Winyah Bay, SC	0.0719 ± 0.0834	RTK-GPS
Rosso, et al. [11]	San Francisco Bay, CA	0.09	Total Station
Wang, et al. [13]	Venice Lagoon, Italy	0.022 ± 0.064	DGPS
Chassereau, et al. [15]	North Inlet-Winyah Bay, SC	0.05 ± 0.28	RTK-GPS
Populus, et al. [16]	Anse de l'Aiguillon, France	0.006 ± 0.10 to 0.01 ± 0.11	DGPS
Schmid, et al. [18]	Charleston, SC	0.153 ± 0.176	Static GPS + Total Station
Hladik and Alber [19]	Sapelo Island, GA	0.03 to 0.25	RTK-GPS
Millard, et al. [21]	Upper Bay of Fundy, Canada	0.30	Adjusted DGPS
Thorne, et al. [23]	San Pablo Bay, CA	0.10 to 0.35	Leveling, RTK-GPS
Medeiros, et al. [25]	Apalachicola, FL	0.61 ± 0.24	RTK-GPS
Fernandez-Nunez, et al. [27]	Odiel, Spain	0.23 ± 0.13 to 0.45 ±0.19	RTK-GPS

B. Impact of Elevation in Marsh Models

Previous studies have explored the influence of elevation on the outcomes of marsh models. Swanson *et al.* [49] applied the Wetland Accretion Model for Ecosystem Resilience (WARMER) [50] to sites across the Pacific Northwest. They found that the initial site elevation was the second most influential variable in determining the persistence of the marsh area with SLR; elevation was second only to the rate of SLR. Applying the marsh equilibrium model (MEM) [32] to marshes in San Francisco Bay [35] also showed that the marsh response to SLR differed based on the initial elevation.

More specifically, there have been studies that examined the impact of error in lidar-derived DEMs. Geselbracht *et al.* [14] applied the sea-level affecting marshes model (SLAMM) [36] using the national elevation dataset and a lidar-derived DEM and found that the resulting habitat distribution area differed by up to 173%. In addition, SLAMM sensitivity to adjusted and unadjusted topography was tested in modeling a microtidal Mediterranean Sea marsh system in Spain [51], which showed significant dependence of the results on the initial elevation and demonstrated the need to adjust the marsh platform for future projections. Buffington *et al.* [52] applied WARMER to adjusted and unadjusted lidar-derived DEMs and found predictions on the timing of marsh loss changed by as much as 30 years. Here, we expand upon these studies, examining under what tidal conditions it is most pressing to adjust lidar-derived DEMs to achieve accurate marsh modeling results.

We have two main goals: first, to contribute to the building body of work documenting the difference between lidar-derived DEMs and RTK measurements in salt marsh systems; second, to examine how these topographic differences impact marsh model results in micro- and mesotidal systems. This article will help inform the increasing number of marsh-model users when it is or is not critical to adjust lidar-derived DEMs.

II. METHODS

Global navigation satellite system (GNSS) RTK data (herein referred to as RTK) were collected from three sites to assess error in lidar-derived DEMs. Two sites from microtidal regions in the NGOM and one from a mesotidal region in Massachusetts were used for modeling based on the availability of hydrodynamic and marsh model results. The lidar-derived DEMs were adjusted

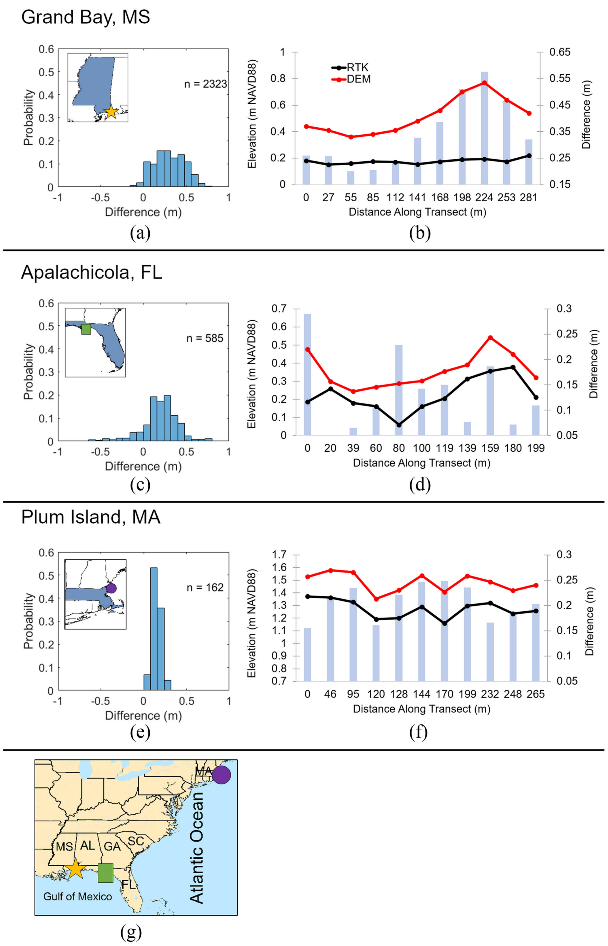

Fig. 1. Magnetization comparison between RTK surveyed elevations (black lines) and lidar-derived DEM elevations (red lines) in (a), (b) Grand Bay, MS, USA, (c), (d) Apalachicola, FL, USA, and (e), (f) Plum Island, MA, USA. Select transects from each survey are shown on the right. The difference (histograms and light blue bars) is calculated as the DEM elevation minus the RTK elevation. Histograms are normalized by probability and the number of samples is given for each. Map insets and (g) show locations of the study sites.

where needed using RTK data of the marsh platform. Both adjusted and unadjusted DEMs were used in the hydro-MEM model [30] to produce marsh coverage maps, as well as inundated regions at high tide. Marsh coverage results generated by hydro-MEM were then compared with available wetland data to assess their agreement.

A. Study Sites

There are two study sites in the NGOM: Apalachicola, FL, USA, and Grand Bay, MS, USA (see Fig. 1). Both sites are microtidal with tide ranges from 0.5 to 1 m [53]. Grand Bay has diurnal tides, while Apalachicola has mixed diurnal tides. Apalachicola Bay is located in the Florida panhandle and is a fluvial shallow estuary protected by barrier islands; it receives the discharge from Apalachicola River, the largest river in discharge in Florida. Historically, Apalachicola Bay provides 90% of Florida's oyster harvest [54]. Grand Bay is a marine-dominated estuary and is not connected to any fluvial source. It consists of several bays and contains barrier islands that protect it from waves from the Gulf of Mexico [55], [56].

The selected mesotidal study site is the Plum Island Estuary located in northern Massachusetts (see Fig. 1). The tides at this estuary, which receives the discharge from Parker and Ipswich rivers, are semidiurnal, and the tidal range is 2.67 m [5]. The spring-neap tide range varies from 2.6 to 3.6 m [57]. Most of the estuary is covered by tidal marsh dominated by *Spartina patens* and *Spartina alterniflora* [5], [57].

B. DEM Adjustment Using RTK Data

The RTK data for Apalachicola were obtained in January 2010; it was collected within the marsh system on an approximately 20 m grid. The RTK data for Grand Bay and Plum Island were provided by Grand Bay national estuarine research reserve (GBNERR) and Plum Island ecosystem long-term ecological research (LTER), respectively, and are in the form of transects within the marsh system. RTK GNSS data using a single base station or virtual reference station solution from a network have typical horizontal and vertical accuracies of 1–3 cm and 2–5 cm, respectively [9], [58].

The DEM for the Apalachicola estuary was provided by Northwest Florida Water Management District and was developed from lidar surveys conducted from May to August 2007. The DEM for Grand Bay was developed using the topographic lidar data acquired by the Mississippi Department of Environmental Quality in 2015 and Mobile County/City of Mobile, Alabama in 2014 [59]. The topographic data for the Plum Island estuary were obtained from the Massachusetts GIS office and were collected from lidar surveys in spring 2011 [60].

Elevations were extracted from the lidar-derived DEMs at all RTK measurement locations. Error is defined as the difference between the RTK measurement and the DEM elevation. Positive values indicate that the lidar-derived elevation is higher than the RTK measurement. To determine outliers, z-scores were calculated and error measurements with a z-score of 3 or greater were deemed outliers and were removed from the dataset.

The collected RTK data were used to adjust the lidar-derived DEM. In Apalachicola, the DEM was first adjusted downward based on an estimation of above-ground biomass density using remote sensing data [25]. This reduced the bias in the DEM by approximately 40%. Since all previous studies mentioned herein agree that the lidar DEM bias increases with denser and taller vegetation, the remaining bias was removed by lowering the DEM by approximately 30 cm at the downstream end (where vegetation is generally denser and taller) and decreasing the adjustment linearly moving upriver (where vegetation is generally sparser) in a northwesterly direction. In Grand Bay, the DEM was adjusted by analyzing the distribution of elevations in areas classified as marsh and adjusting them by numerically restricting their range to the upper portion of the local hydroperiod, extended to account for microtopography [61]. This preserved the natural variability in the DEM while removing the lidar bias. Note that the lidar DEM for Plum Island was not adjusted, for reasons explained in Section III.

C. Hydrodynamic-Marsh Model

To investigate the topographic uncertainty effect in marsh model results, we used hydro-MEM. Unlike other commonly used models, such as SLAMM or MEM, that use constant water level, hydro-MEM is a dynamic model and incorporates highly accurate modeled water level changes within the creeks and marsh platform [62]–[64]. The hydro-MEM model [30] was developed to couple a hydrodynamic model and a parametric marsh model to capture the biological feedback in marsh systems. This integrated model incorporates the ADvanced CIRCulation (ADCIRC) finite-element code [65] that solves the shallow-water equations on an unstructured triangular mesh. The ADCIRC component of the model yields hydrodynamic parameters as inputs for the MEM [32] that produce marsh productivity in the form of biomass density. MEM formulates biomass density of a salt marsh as a parabolic function of MHW and marsh platform elevation

$$B = \alpha D^2 + bD + c \tag{1}$$

$$D = \text{MHW} - \text{Elevation.} \tag{2}$$

Constants a, b, and c are unique for individual estuaries [66] and were derived from previous bioassay experiments in Apalachicola [67], Grand Bay [61], and Plum Island [5]. Equation (2) further highlights the important role of accurate water levels and elevation in the biomass calculation.

D. Validation and Adjustment Criteria

A hydro-MEM simulation was run for each study site with the unadjusted lidar-derived DEM. The hydro-MEM results in the form of biomass density (1) were converted to marsh coverage by categorizing any biomass value above zero as marsh in an ArcGIS raster cell. The resulting marsh coverage estimations in the form of polygon shapefiles are then compared with the wetland region shapefile data of the National Wetland Inventory (NWI) [2], [68]. The agreement regions are the areas that the model successfully produced marsh coverage compared with NWI data. In addition to agreement percentage, we calculated Cohen's Kappa to measure the agreement with the NWI data [69]–[71]. Cohen's Kappa (*Kappa* number) is used to measure agreement between categorical variables and is often used to assess agreement between maps [71], [72]. Kappa is preferable to direct comparisons because it accounts for agreement due to random chance; a value of 1 shows a perfect agreement, and a value of 0 is disagreement. A value above 0.6 shows "substantial agreement" [70], or in another measuring table, a value above 0.55 is called "good agreement" [71]. Therefore, for this study, if Kappa was less than 0.55, we deemed it necessary to adjust the lidar-derived DEM, and we reran hydro-MEM with the adjusted DEM.

III. Results and Discussion

Comparisons of the elevations in the DEMs and the RTK measurements confirm the positive bias in lidar-derived DEMs (see Fig. 1). The error range in the study sites was all in agreement with the error ranges presented in Table I.

In Grand Bay [see Fig. 1(a) and (b)], the average error is 30 cm, which is 84% of the tide range (35.8 cm) and is approximately 1.4 times larger than the MHW value of 21 cm NAVD88 (Dauphin Island NOAA Station 8735180). In addition, the selected transect demonstrates the variability in lidar accuracy. From 141 to 281 m along the transect, the lidar-derived DEM contains a false ridge approximately 50 cm tall, which could impact the modeling of the flow patterns and biomass density at the site.

In Apalachicola [see Fig. 1(c) and (d)], the error ranged from −60 to 80 cm with a mean of 20 cm. The negative error indicates higher RTK than lidar-derived elevation; these points tend to be located in mudflat or creek regions, where geomorphological processes can change the elevation. In the lower river marshes, measured by Medeiros *et al.* [25], the lidar-derived DEM error ranged from −60 to 160 cm with a mean of 61 cm, as listed in Table I. Apalachicola Bay has an MHW elevation of 23 cm NAVD88 and a tide range of 34 cm (Apalachicola NOAA Station 8728690).

In microtidal environments (tide ranges $<$ 50 cm), such as those found in NGOM, these errors represent a substantial percentage of the tidal range. In addition to the problem of producing an unrealistic marsh hydroperiod, lidar-derived DEMs also distort the microtopography and creek structure of the marsh. In most cases, the lidar-derived DEM smooths out small creeks and impoundments that contain emergent marsh grasses, influencing the inundation regime and the subsequent projections of vegetation zonation and biomass productivity [19], [73], [74].

The results from Plum Island show that the error is negligible compared with the tide range. The maximum amount of lidar-derived elevation error is 29 cm, and the average is 15 cm [see Fig. 1(e) and (f)]. This average error is 5.2% of the tide range (2.89 m) and 11% of the MHW value of 1.32 m NAVD88 (Boston NOAA Station 8443970). Although the sample size for this site is smaller, the error is more consistent with a standard deviation of 5 cm.

The errors in the marsh model results can be explained in part by incorrect hydroperiod. The hydroperiod for which a species of salt marsh vegetation can flourish is typically narrow [75] and relatively small differences in marsh surface elevation can significantly affect inundation patterns and the spatial distribution of vegetation species [19], [74]. Fig. 2 compares inundation depth range for tidally inundated regions in the microtidal system of Grand Bay [see Fig. 2(a)] with the mesotidal system of Plum Island [see Fig. 2(b)]. Equation (1), with the site-specific coefficients, is plotted against the range of inundation where marsh is productive (see Fig. 2, top). The brown and yellow areas indicate low inundation depth, which results in a high marsh with low productivity, and the blue regions show high inundation depths in low elevation marsh that results in low productivity marsh. The green areas contain the optimum inundation depth that creates the most productive marsh. The elevation error could occur anywhere on the marsh platform, and therefore, any point on the x-axis of the parabola can be miscalculated. An example of a plausible 25 cm error range is shown in the figure (red arrow). In Grand Bay, this amount of error could cause a major change in inundation depth calculation and consequently, a high productivity point (maximum of the parabola) can be misclassified as being outside of the tide range (change the biomass density from 2000 to 0 gr/m^2·yr). However, in Plum Island, the marsh is productive within a 175 cm inundation depth

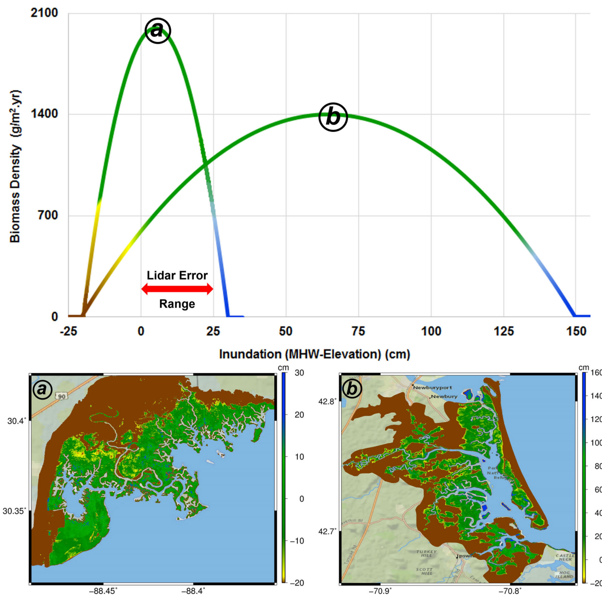

Fig. 2. Tidal inundation depth in a microtidal (Grand Bay, (a) in top and bottom graphic) and mesotidal (Plum Island, (b) in top and bottom graphic) estuary. The green area demonstrates inundation depth that is conducive to productive marsh regions. Yellow and brown indicate lower inundation depth that resulted in low-productivity high elevation marshes and blue indicates where high inundation depth combined with low elevation results in a low productivity marsh.

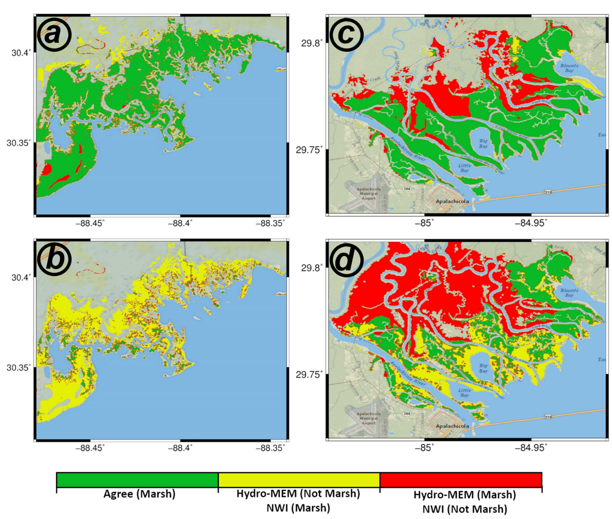

Fig. 3. Comparison of the hydro-MEM model results with NWI [2] data using RTK-adjusted (top figures) and lidar-derived DEM (bottom figures) in (a), (b) Grand Bay and (c), (d) Apalachicola. The maps are classified in green (model and data both show marsh), yellow (data indicate as marsh but model did not produce marsh), and red (the model calculation demonstrates marsh but the data disagree). This qualitative assessment indicates the value of RTK-based adjustments in these microtidal systems.

range, and 25 cm of error within this range has minimal effect in calculating inundation depth and biomass density.

The hydro-MEM results at Apalachicola [67], Grand Bay [61], and Plum Island were compared with the NWI data to examine the effects of lidar-derived topographic error perturbation in the model results. The results were categorized into three groups: agreement, where the model results and NWI data both show marsh (Fig. 3, colored in green); Type I (false positive) disagreement, where the model calculated marsh but the NWI data did not show marsh (Fig. 3, colored in red); and Type II disagreement (false negative), where the NWI data show marsh, but the model did not capture it (Fig. 3, colored in yellow). A comparison of the adjusted marsh platform model in Grand Bay with NWI data [see Fig. 3(a)] indicated that 70% of the area is in agreement, and the Kappa value is 0.77. These values increase to 82% and 0.83, respectively, if constrained to the GBNERR region [61]. In contrast, the vast yellow region in Fig. 3(b) indicates that the model underestimates the marsh coverage due to the topographic error in the unadjusted DEM. Using the original DEM in the model captured just 8% of the marsh region [green area in Fig. 3(c)], and the Kappa value is 0.1, which is categorized as "very poor agreement" [71]. This estuary is a marine-dominated estuary and is not connected to any river inflow. As a result, the main source of error in this site is the direct effect of topographic error in the biomass density calculation. However, in fluvial estuaries where a river and tidal flows meet in complex creek networks within wetlands, the topographic error impacts the water level in addition to the platform elevation component of the hydroperiod calculation.

Apalachicola is a canonical example of a fluvial microtidal system. Employing the lidar-derived DEM resulted in 24% agreement in marsh coverage [green regions in Fig. 3(d)] with a Kappa value of 0.1. The low Kappa value with better agreement percentage compared with Grand Bay is due to the large area of false marsh, as shown by red in Fig. 3(d). This increase in marsh generation in the forested region can be explained by nonlinear perturbation of the topographic error in the model. The topographic error effect in marsh calculations of the fluvial estuary can be categorized into two groups. The first topographic error effect is the direct influence of topography in marsh productivity calculation in the MEM formula [see (1) and (2)]. The second effect is a result of the nonlinear error perturbation through incorrect topography input in ADCIRC, the hydrodynamic model component. The incorrect input in ADCIRC can change the variations in MHW within the creeks and across the marsh system. This nonlinear error in the MHW calculation affects the biomass density variable in (2) and, consequently, the marsh productivity results. To fix this problem, an elevation adjustment method [25] was applied, the input DEM was updated, and consequently, the model agreement increased to 57% [see Fig. 3(c)] with a Kappa value of 0.6.

Although the error exists in the Plum Island elevation measurements, it is less significant compared with the NGOM sites. While the elevation error could influence species delineation, as small variations in topography can lead to a different vegetative community, it does not change marsh coverage results from the hydro-MEM model. The comparison between NWI data and the hydro-MEM marsh coverage from the original lidar-derived DEM showed 67% agreement with a Kappa value of 0.73. This value for Kappa, as explained in the methods section, suggests "substantial agreement and there is no need for topographic adjustment. Based on these results, lidar DEM error can be reasonably neglected for marsh modeling in meso- and macrotidal systems, but it is critical to account for it in microtidal systems clearances.

IV. Conclusion

RTK data from marsh platforms in two microtidal and one mesotidal estuaries were compared with lidar-derived DEMs. The measurements confirmed the topographic error in lidar-derived DEMs, found in other studies. For the two microtidal sites, the DEMs were adjusted using the collected RTK data, and marsh coverage projections for all three sites were modeled using hydro-MEM to investigate the effect of nonlinear error perturbations. Marsh coverage misclassification is directly caused by incorrect elevations relative to tidal data for the two microtidal estuaries and indirectly by the generation of incorrect tidal data in the fluvial system. The marsh coverage projections at two microtidal sites using lidar-derived DEM showed "very poor agreement" (Kappa value of 0.1) when compared with NWI data. However, employing an RTK-adjusted topography increased the result to "substantial agreement" with Kappa values of 0.6 and 0.77, respectively. The marine-dominated estuary and its simple creek network reduced the impact of topography in modeling tidal data. In contrast, the water levels in the complex creek network in the fluvial estuary were affected by incorrect topography and produced a large area of false marsh. Although a similar range of error in lidar-derived topography in the mesotidal system exists, the Cohen's Kappa value using original lidar-derived DEM is 0.73. This result is due to the error being low in comparison with the tide range, the generalized approach to salt marsh biomass productivity, and to the robust present-day nature of this mesotidal system. It is incumbent on researchers throughout the world to recognize these potential elevation errors within marsh systems. It is particularly important to have correct initial elevations since future SLR assessments build upon the present-day analyses and when a marsh system transitions in productivity the relatively low topographic errors will become noteworthy, regardless of whether the system is micro-, meso-, or macrotidal.

Acknowledgment

The authors would like to thank ANERR, GBERR, and Plum Island Ecosystem LTER staffs, especially W. Underwood and Dr. J. Pitchford, for providing useful data and for their continuous help and support.

References

[1] J. Towns *et al.*, "XSEDE: Accelerating scientific discovery," *Comput. Sci. Eng.*, vol. 16, no. 5, pp. 62–74, Sep./Oct. 2014.

[2] L. M. Cowardin, V. Carter, F. C. Golet, and E. T. LaRoe, *Classification of Wetlands and Deepwater Habitats of the United States*. Falls Church, VA, USA: Fish and Wildlife Service, U.S. Dept. Interior, 1979.

[3] J. T. Morris *et al.*, "Integrating LIDAR elevation data, multi-spectral imagery and neural network modelling for marsh characterization," *Int. J. Remote Sens.*, vol. 26, pp. 5221–5234, 2005.

[4] K. B. Gedan, M. L. Kirwan, E. Wolanski, E. B. Barbier, and B. R. Silliman, "The present and future role of coastal wetland vegetation in protecting shorelines: Answering recent challenges to the paradigm," *Climatic Change*, vol. 106, pp. 7–29, 2010.

[5] J. T. Morris, K. Sundberg, and C. Hopkinson, "Salt marsh primary production and its responses to relative sea level and nutrients in estuaries at Plum Island, Massachusetts and North Inlet, South Carolina, USA," *Oceanography*, vol. 26, pp. 78–84, 2013.

[6] F. Daiber, "Salt marsh animals: Distributions related to tidal flooding, salinity and vegetation," in *Wet Coastal Ecosystems*, V. J. Chapman, Ed., vol. 1. Amsterdam, The Netherlands: Elsevier, 1977, pp. 79–108.

[7] P. M. Halpin, "Habitat use by an intertidal salt-marsh fish: Trade-offs between predation and growth," *Mar. Ecol. Prog. Ser.*, vol. 198, pp. 203–214, 2000.

[8] I. Möller and T. Spencer, "Wave dissipation over macro-tidal saltmarshes: Effects of marsh edge typology and vegetation change," *J. Coastal Res.*, vol. 36, pp. 506–521, 2002.

[9] J. M. Montane and R. Torres, "Accuracy assessment of LIDAR saltmarsh topographic data using RTK GPS," *Photogrammetric Eng. Remote Sens.*, vol. 72, pp. 961–967, 2006.

[10] C. C. Shepard, C. M. Crain, and M. W. Beck, "The protective role of coastal marshes: A systematic review and meta-analysis," *PLOS One*, vol. 6, 2011, Art. no. e27374.

[11] P. H. Rosso, S. L. Ustin, and A. Hastings, "Use of lidar to study changes associated with Spartina invasion in San Francisco Bay marshes," *Remote Sens. Environ.*, vol. 100, pp. 295–306, 2006.

[12] J. D. Woodruff, J. L. Irish, and S. J. Camargo, "Coastal flooding by tropical cyclones and sea-level rise," *Nature*, vol. 504, pp. 44–52, 2013.

[13] C. Wang, M. Menenti, M.-P. Stoll, A. Feola, E. Belluco, and M. Marani, "Separation of ground and low vegetation signatures in LiDAR measurements of salt-marsh environments," *IEEE Trans. Geosci. Remote Sens.*, vol. 47, no. 7, pp. 2014–2023, Jul. 2009.

[14] L. Geselbracht, K. Freeman, E. Kelly, D. R. Gordon, and F. E. Putz, "Retrospective and prospective model simulations of sea level rise impacts on Gulf of Mexico coastal marshes and forests in Waccasassa Bay, Florida," *Climatic Change*, vol. 107, pp. 35–57, 2011.

[15] J. E. Chassereau, J. M. Bell, and R. Torres, "A comparison of GPS and lidar salt marsh DEMs," *Earth Surface Processes Landforms*, vol. 36, pp. 1770–1775, 2011.

[16] J. Populus, G. Barreau, J. Fazilleau, M. Kerdreux, and J. L. Yavanc, "Assessment of the LIDAR topographic technique over a coastal area," in *Proc. CoastGIS*, vol. 1, 2011, p. 4.

[17] E. B. Watson *et al.*, "Nutrient enrichment and precipitation changes do not enhance resiliency of salt marshes to sea level rise in the Northeastern U.S.," *Climatic Change*, vol. 125, pp. 501–509, 2014.

[18] K. A. Schmid, B. C. Hadley, and N. Wijekoon, "Vertical accuracy and use of topographic LIDAR data in coastal marshes," *J. Coastal Res.*, vol. 27, pp. 116–132, 2011.

[19] C. Hladik and M. Alber, "Accuracy assessment and correction of a LIDAR-derived salt marsh digital elevation model," *Remote Sens. Environ.*, vol. 121, pp. 224–235, 2012.

[20] C. T. Friedrichs and J. E. Perry, "Tidal salt marsh morphodynamics: A synthesis," *J. Coastal Res.*, no. 27 (Special Issue), pp. 7–37, 2001.

[21] K. Millard, A. M. Redden, T. Webster, and H. Stewart, "Use of GIS and high resolution LiDAR in salt marsh restoration site suitability assessments in the upper Bay of Fundy, Canada," *Wetlands Ecol. Manage.*, vol. 21, pp. 243–262, 2013.

[22] M. L. Kirwan, G. R. Guntenspergen, A. D'Alpaos, J. T. Morris, S. M. Mudd, and S. Temmerman, "Limits on the adaptability of coastal marshes to rising sea level," *Geophys. Res. Lett.*, vol. 37, 2010, Art. no. L23401, doi: 10.1029/2010GL045489.

[23] K. M. Thorne, D. L. Elliott-Fisk, G. D. Wylie, W. M. Perry, and J. Y. Takekawa, "Importance of biogeomorphic and spatial properties in assessing a tidal salt marsh vulnerability to sea-level rise," *Estuaries Coasts*, vol. 37, pp. 941–951, 2014.

[24] K. Freeman, L. Geselbracht, D. Gordon, E. Kelly, and L. Racevskis, "Understanding future sea level rise impacts on coastal wetlands in the Apalachicola Bay regions of Flopride's Gulf Coast," Florida Department of Environmental Protection Agreement No. CM112. The Nature Conservancy for Florida Department of Environmental Protection, Florida Coastal Management Program, Tallahassee, Florida, 2012.

[25] S. Medeiros, S. Hagen, J. Weishampel, and J. Angelo, "Adjusting lidar-derived digital terrain models in coastal marshes based on estimated aboveground biomass density," *Remote Sens.*, vol. 7, pp. 3507–3525, 2015.

[26] I. H. Townend, C. Fletcher, M. Knaapen, and S. K. Rossington, "A review of salt marsh dynamics," *Water Environ. J.*, vol. 25, pp. 477–488, 2010.

[27] M. Fernandez-Nunez, H. Burningham, and J. O. Zujar, "Improving accuracy of LiDAR-derived digital terrain models for saltmarsh management," *J. Coastal Conservation*, vol. 21, pp. 209–222, Feb. 2017.

[28] D. J. Reed, "The impact of sea-level rise on coastal salt marshes," *Prog. Phys. Geography*, vol. 14, pp. 465–481, Dec. 1990.

[29] S. C. Hagen, J. T. Morris, P. Bacopoulos, and J. F. Weishampel, "Sea-level rise impact on a salt marsh system of the lower St. Johns river," *J. Waterway Port Ocean Eng.*, vol. 139, pp. 118–125, 2012.

[30] K. Alizad *et al.*, "A coupled, two-dimensional hydrodynamic-marsh model with biological feedback," *Ecol. Model.*, vol. 327, pp. 29–43, 2016.

[31] M. L. Kirwan and A. B. Murray, "A coupled geomorphic and ecological model of tidal marsh evolution," *Proc. Nat. Acad. Sci.*, vol. 104, pp. 6118–6122, Apr. 2007.

[32] J. T. Morris, P. V. Sundareshwar, C. T. Nietch, B. Kjerfve, and D. R. Cahoon, "Responses of coastal wetlands to rising sea level," *Ecology*, vol. 83, pp. 2869–2877, 2002.

[33] S. M. Mudd, S. Fagherazzi, J. T. Morris, and D. J. Furbish, "Flow, sedimentation, and biomass production on a vegetated salt marsh in South Carolina: Toward a predictive model of marsh morphologic and ecologic evolution," in *The Ecogeomorphology of Tidal Marshes*, vol. 59. Hoboken, NJ, USA: Wiley, 2004, pp. 165–188.

[34] G. Mariotti and S. Fagherazzi, "A numerical model for the coupled long-term evolution of salt marshes and tidal flats," *J. Geophys. Res.*, vol. 115, 2010, Art. no. F01004, doi: 10.1029/2009JF001326.

[35] L. M. Schile, J. C. Callaway, J. T. Morris, D. Stralberg, V. T. Parker, and M. Kelly, "Modeling tidal marsh distribution with sea-level rise: Evaluating the role of vegetation, sediment, and upland habitat in marsh resiliency," *Plos One*, vol. 9, 2014, Art. no. e88760.

[36] R. A. Park, T. V. Armentano, and C. L. Cloonan, "Predicting the effects of sea level rise on coastal wetlands," in *Effects Changes Stratospheric Ozone Global Climate*, vol. 4, 1986, pp. 129–152.

[37] D. R. Cahoon and D. J. Reed, "Relationships among marsh surface topography, hydroperiod, and soil accretion in a deteriorating Louisiana salt marsh," *J. Coastal Res.*, vol. 11, pp. 357–369, 1995.

[38] I. Warren Pinnacle Consulting, "Application of the sea-level affecting marshes model (SLAMM 6) to merritt island NWR," Waitsfield, Burlington, VT, USA, Dec. 2011.

[39] R. A. Park, M. S. Trehan, P. W. Mausel, R. C. Howe, and J. G. Titus, "The effects of sea level rise on us coastal wetlands and lowlands," Office Policy, Planning Eval., U.S. Environ. Protection Agency, Washington, D.C., USA, Agreement CR814578-01, 1989.

[40] T. Kana, W. Eiser, B. Baca, and M. Williams, "Potential impacts of sea level rise on wetlands around southcentral New Jersey," Report U.S. Environ. Protection Agency, Washington, D.C., USA, vol. 30, 1985.

[41] J. S. Clough, R. A. Park, and R. Fuller, "SLAMM 6 beta technical documentation," Waitsfield, Burlington, VT, USA, 2010.

[42] C. Craft *et al.*, "Forecasting the effects of accelerated sea-level rise on tidal marsh ecosystem services," *Front. Ecol. Environ.*, vol. 7, pp. 73–78, 2009.

[43] N. R. Goodwin, N. C. Coops, and D. S. Culvenor, "Assessment of forest structure with airborne LiDAR and the effects of platform altitude," *Remote Sens. Environ.*, vol. 103, pp. 140–152, 2006.

[44] C. E. Parrish, J. N. Rogers, and B. R. Calder, "Assessment of waveform features for lidar uncertainty modeling in a coastal salt marsh environment," *IEEE. Geosci. Remote Sens. Lett.*, vol. 11, no. 2, pp. 569–573, Feb. 2014.

[45] S. Silvestri, M. Marani, and A. Marani, "Hyperspectral remote sensing of salt marsh vegetation, morphology and soil topography," *Phys. Chem. Earth, A/B/C*, vol. 28, pp. 15–25, 2003.

[46] F. Andrade, J. Blanton, M. A. Ferreira, and J. Amft, "Developments in salt marsh topography analysis using airborne infrared photography," in *Remote Sensing and Modeling: Advances in Coastal and Marine Resources*, vol. 9, C. W. Finkl and C. Makowski, Eds. New York, NY, USA: Springer, 2014, pp. 317–331.

[47] R. S. Eon *et al.*, "Retrieval of salt marsh above-ground biomass from high-spatial resolution hyperspectral imagery using PROSAIL," *Remote Sens.*, vol. 11, 2019, Art. no. 1385.

[48] D. F. Maune, Ed., *Digital Elevation Model Technologies and Applications: The DEM Users Manual*, 2nd ed. Bethesda, MD, USA: Am. Soc. Photogrammetry Remote Sensing, 2007.

[49] K. M. Swanson, J. Z. Drexler, C. C. Fuller, and D. H. Schoellhamer, "Modeling tidal freshwater marsh sustainability in the Sacramento–San Joaquin Delta under a broad suite of potential future scenarios," *San Francisco Estuary Watershed Sci.*, vol. 13, no. 1, 2015, doi: 10.15447/sfews.2015v13iss1art3.

[50] K. M. Swanson *et al.*, "Wetland accretion rate model of ecosystem resilience (WARMER) and its application to habitat sustainability for endangered species in the san francisco estuary," *Estuaries Coasts*, vol. 37, pp. 476–492, Mar. 2014.

[51] M. Fernandez-Nunez, H. Burningham, P. Díaz-Cuevas, and J. Ojeda-Zújar, "Evaluating the response of Mediterranean-Atlantic saltmarshes to sea-level rise," *Resources*, vol. 8, 2019, Art. no. 50.

[52] K. J. Buffington, B. D. Dugger, K. M. Thorne, and J. Y. Takekawa, "Statistical correction of lidar-derived digital elevation models with multispectral airborne imagery in tidal marshes," *Remote Sens. Environ.*, vol. 186, pp. 616–625, 2016.

[53] H. E. Seim, B. Kjerfve, and J. E. Sneed, "Tides of Mississippi Sound and the adjacent continental shelf," *Estuarine, Coastal Shelf Sci.*, vol. 25, pp. 143–156, 1987.

[54] "Apalachicola national estuarine research reserve management plan," Florida Dept. Environ. Protection, Tallahassee, FL, USA, 2013.

[55] "Grand Bay national estuarine research reserve management plan 2013-2018," Mississippi Dept.Marine Resources, Grand Bay Nat. Estuarine Res. Reserve, Moss Point, MS, USA, 2013.

[56] R. A. Morton, "Historical changes in the Mississippi-Alabama barrier-island chain and the roles of extreme storms, sea level, and human activities," *J. Coastal Res.*, vol. 24, pp. 1587–1600, 2008.

[57] J. J. Vallino and C. S. Hopkinson, Jr., "Estimation of dispersion and characteristic mixing times in plum island sound estuary," *Estuarine, Coastal Shelf Sci.*, vol. 46, pp. 333–350, 1998.

[58] G. R. Hu, H. S. Khoo, P. C. Goh, and C. L. Law, "Development and assessment of GPS virtual reference stations for RTK positioning," *J. Geodesy*, vol. 77, pp. 292–302, 2003.

[59] Nat. Ocean. Atmos. Admin. Digit. Coast Data Access Viewer, "Custom processing of '2014 Mobile County Lidar (AL)'," NOAA Office for Coastal Management, 2014. [Online]. Available: https://coast.noaa.gov/dataviewer

[60] "Lidar terrain data," Bureau Geographic Inf., Commonwealth Massachusetts, Executive Office Technol. Secur. Services, 2011. [Online]. Available: (http://www.mass.gov/anf/research-and-tech/it-serv-and-support/application-serv/office-of-geographic-information-massgis/datalayers/layerlist.html

[61] K. Alizad *et al.*, "Dynamic responses and implications to coastal wetlands and the surrounding regions under sea level rise," *Plos One*, vol. 13, 2018, Art. no. e0205176.

[62] M. V. Bilskie, S. C. Hagen, S. C. Medeiros, A. T. Cox, M. Salisbury, and D. Coggin, "Data and numerical analysis of astronomic tides, wind-waves, and hurricane storm surge along the northern Gulf of Mexico," *J. Geophy. Res., Oceans*, vol. 121, pp. 3625–3658, 2016.

[63] D. L. Passeri, S. C. Hagen, N. G. Plant, M. V. Bilskie, S. C. Medeiros, and K. Alizad, "Tidal hydrodynamics under future sea level rise and coastal morphology in the Northern Gulf of Mexico," *Earth's Future*, vol. 4, pp. 159–176, 2016.

[64] M. V. Bilskie *et al.*, "Dynamic simulation and numerical analysis of hurricane storm surge under sea level rise with geomorphologic changes along the northern Gulf of Mexico," *Earth's Future*, vol. 4, pp. 177–193, 2016.

[65] R. A. Luettich, Jr., and J. Westerink, "Formulation and numerical implementation of the 2D/3D ADCIRC finite element model version 44. XX: R. Luettich," 2004. [Online]. Available: https://adcirc.org/files/2018/11/adcirc_theory_2004_12_08.pdf

[66] J. T. Morris, "Ecological engineering in intertidial saltmarshes," *Hydrobiologia*, vol. 577, pp. 161–168, 2007.

[67] K. Alizad, S. C. Hagen, J. T. Morris, S. C. Medeiros, M. V. Bilskie, and J. F. Weishampel, "Coastal wetland response to sea-level rise in a fluvial estuarine system," *Earth's Future*, vol. 4, pp. 483–497, 2016.

[68] National Fish Wildlife Service, "Mississippi coast updates NWI based imagery from 2006 and 2007," NWI, 2009. [Online]. Available: https://www.fws.gov/wetlands/Data/SupMapInf/R04Y08P10.pdf

[69] J. Cohen, "A coefficient of agreement for nominal scales," *Educ. Psychol. Meas.*, vol. 20, pp. 37–46, 1960.

[70] J. R. Landis and G. G. Koch, "The measurement of observer agreement for categorical data," *Biometrics*, vol. 33, pp. 159–174, 1977.

[71] R. A. Monserud and R. Leemans, "Comparing global vegetation maps with the Kappa statistic," *Ecol. Model.*, vol. 62, pp. 275–293, 1992.

[72] B. C. Timm and K. McGarigal, "Fine-scale remotely-sensed cover mapping of coastal dune and salt marsh ecosystems at Cape Cod National Seashore using Random Forests," *Remote Sens. Environ.*, vol. 127, pp. 106–117, 2012.

[73] L. Morzaria-Luna, J. C. Callaway, G. Sullivan, and J. B. Zedler, "Relationship between topographic heterogeneity and vegetation patterns in a Californian salt marsh," *J. Vegetation Sci.*, vol. 15, pp. 523–530, 2004.

[74] A. D' Alpaos, "The mutual influence of biotic and abiotic components on the long-term ecomorphodynamic evolution of salt-marsh ecosystems," *Geomorphol.*, vol. 126, pp. 269–278, 2011.

[75] D. Stralberg *et al.*, "Evaluating tidal marsh sustainability in the face of sea-level rise: A hybrid modeling approach applied to San Francisco bay," *Plos One*, vol. 6, 2011, Art. no. e27388.

Karim Alizad was born in Rasht, Iran, in 1981. He received his Ph.D. in civil engineering at the University of Central Florida (UCF), in 2016 and worked two years as a Postdoctoral Research Associate with the Center for Coastal Resiliency (CCR) at Louisiana State University (LSU). He has earned a B.S. in Mechanical Engineering from Semnan University, in 2005; an M.S. in energy conversion from the University of Tehran, in 2009; and completed his second M.S. in Mechanical Engineering at the University of California, Riverside (UCR), in 2011.

He is currently a research assistant professor in the Baruch Institute for Marine and Coastal Sciences at the University of South Carolina. His research is focused on the effects of climate change and sea level rise on coastal ecosystems and coupling field collected data with large-scale hydrodynamic models.

Stephen C. Medeiros was born in Massachusetts, USA, in 1977. He received the bachelor's and master's degrees in civil engineering from the Florida Institute of Technology, Melbourne, FL, USA, in 1999 and 2002, respectively, and the Ph.D. degree in civil engineering from the University of Central Florida, Orlando, FL, USA, in 2012.

He is currently an Assistant Professor with the Department of Civil Engineering, Embry-Riddle Aeronautical University, Daytona Beach, FL, USA. His research interests include the fusion of remote sensing, field measurements, and computer modeling for natural hazard applications.

Dr. Medeiros is a Registered Professional Engineer in the State of Florida.

Madeline R. Foster-Martinez was born in Louisiana, USA, in 1989. She received the bachelor's degree in civil engineering from The Cooper Union, New York, NY, USA, in 2012, and the master's and Ph.D. degrees in civil and environmental engineering from the University of California, Berkeley, CA, USA, in 2013 and 2017, respectively.

She is currently a Research Associate with Pontchartrain Institute for Environmental Sciences, The University of New Orleans, New Orleans, LA, USA. Her research interests include the integration of built infrastructure and ecologic processes in coastal settings.

Scott C. Hagen was born in Iowa, USA, in 1961. He received the bachelor's degree in civil engineering from the University of Iowa, Iowa City, IA, USA, in 1993, and the Ph.D. degree in civil engineering from the University of Notre Dame, Notre Dame, IN, USA, in 1998.

He is currently a Professor with the Department of Civil and Environmental Engineering, Louisiana State University, Baton Rouge, LA, USA, and holds the John P. Laborde Endowed Chair for Sea Grant Research and Technology Transfer. He also has an appointment with the LSU Center for Computation and Technology, Baton Rouge, and is a Fellow of the LSU Coastal Studies Institute, Baton Rouge. He spent more than 17 years with the University of Central Florida, Orlando, FL, USA, where he established the internationally recognized CHAMPS Laboratory. His research interests include coastal hydroscience and engineering, high-performance computational modeling of ocean, coastal, and inland astronomical, and meteorological tides and flows.

Prof. Hagen is a Registered Professional Engineer in the State of Florida and is a Diplomate of both Coastal and Water Resources Engineering. He is a past member of the Board of Governors for the ASCE/Coasts, Oceans, Ports, and Rivers Institute and he was elected as a Fellow of the American Society of Civil Engineers in 2014.